



## Cytoskeletal motor-driven active self-assembly in *in vitro* systems

A. T. Lam,<sup>a</sup> V. VanDelinder,<sup>b</sup> A. M. R. Kabir,<sup>c</sup> H. Hess,<sup>a\*</sup> G. D. Bachand<sup>b\*</sup> and A. Kakugo<sup>c,d\*</sup>

Received 00th January 20xx,  
Accepted 00th January 20xx

DOI: 10.1039/x0xx00000x

[www.rsc.org/](http://www.rsc.org/)

Molecular motor-driven self-assembly has been an active area of soft matter research for the past decade. Because molecular motors transform chemical energy into mechanical work, systems which employ molecular motors to drive self-assembly processes are able to overcome kinetic and thermodynamic limits on assembly time, size, complexity, and structure. Here, we review the progress in elucidating and demonstrating the rules and capabilities of motor-driven active self-assembly. We focus on the types of structures created and the degree of control realized over these structures, and discuss the next steps necessary to achieve the full potential of this assembly mode which complements robotic manipulation and passive self-assembly.

### Introduction

Self-assembly is the process through which discrete components spontaneously organize and form structures,<sup>1, 2</sup> and may be divided into two classes: passive and active.<sup>1, 3, 4</sup> While passive self-assembly relies on thermal fluctuations to drive diffusive processes by which building blocks move into place, active self-assembly utilizes non-thermal energy to transport the isolated building blocks. Active self-assembly has long been of interest as a means to build structures not achievable through traditional, passive self-assembly or fabrication methods.<sup>1, 3</sup> By harnessing external sources of energy, active self-assembly processes are able to overcome the speed limitations of diffusion-driven “passive” self-assembly and are also able to form non-equilibrium structures (Figure 1).<sup>4</sup>

The most compelling examples of the complexity realizable through active self-assembly are biological organisms, which are composed of and are themselves intricate machines capable of storing, processing, and acting on information. For example, the fertilization of oocytes by sperm cells is critically dependent on the active movement of the sperm and the distribution of chromosomes during mitosis relies on directed transport driven by depolymerizing microtubules. It is convenient to employ these already designed and functional biological units to study active self-assembly.

While active self-assembly can be studied at the macroscale,<sup>5-8</sup> the contrast with passive self-assembly is most instructive in nano- and microscale systems where both active and passive self-assembly mechanisms can be utilized. In particular, biological molecular motors have been used extensively in model systems to study active self-assembly processes.<sup>4, 9-11</sup> These motor proteins cyclically convert

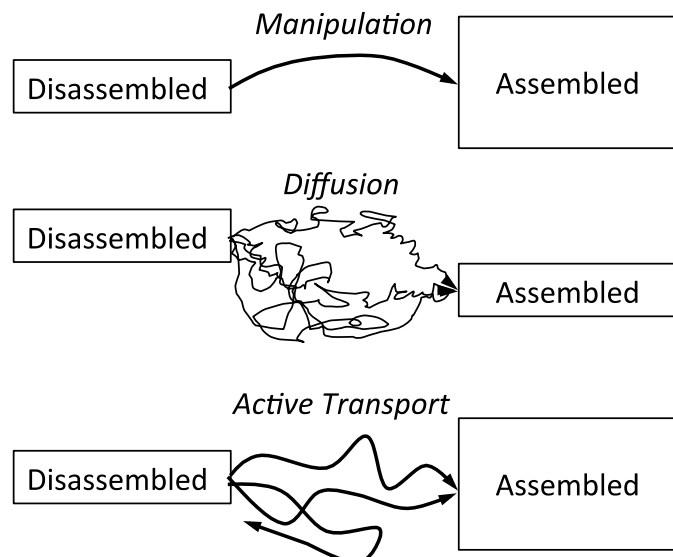


Figure 1: The evolution of a system from a “disassembled” to an “assembled” state can be brought about by direct manipulation of the building blocks as in robotics, by a passive self-assembly process where the relocation of the building blocks is driven by diffusion and can only result in a lower energy structure, and by active self-assembly which combines an active, energy-consuming transport process with an absence of control over the movement.

<sup>a</sup> Columbia University, Department of Biomedical Engineering, 351 Engineering Terrace, 1210 Amsterdam Avenue, MC 8904, New York, NY 10027, USA.

<sup>b</sup> Sandia National Laboratories, Nanosystems Synthesis/Analysis Dept., Albuquerque, NM, USA

<sup>c</sup> Faculty of Science, Hokkaido University, Sapporo 060-0810, Japan.

<sup>d</sup> Graduate School of Chemical Sciences and Engineering, Hokkaido University, Sapporo 060-0810, Japan.

\* Corresponding authors: [hess@columbia.edu](mailto:hess@columbia.edu), [gdbacha@sandia.gov](mailto:gdbacha@sandia.gov), [kakugo@sci.hokudai.ac.jp](mailto:kakugo@sci.hokudai.ac.jp)

chemical energy, typically in the form of ATP, into mechanical work. The motor proteins employed in these *in vitro* experiments on self-assembly move along their associated cytoskeletal filament. However, if the motors are held in place as is often the case, then ATPase activity of the motor results in translational motion of the filaments, which is known as the gliding assay geometry (Figure 2).

In a typical gliding assay, molecular motors are adsorbed to the surface of a substrate, i.e. the experimental flow cell, and propel their associated filaments in a persistent random walk along the substrate surface.<sup>12, 13</sup> The cytoskeletal filaments are polar, having a plus-end and a minus-end, and molecular motors move unidirectionally along the filament towards either the plus- or minus-end depending on the type of motor. Thus, if there is only one species of motor on the surface, the motors will work in concert with one another.

The gliding assay can be modified such that attractive interactions can be induced between motor-propelled filaments by the inclusion of cross-linkers. Fluorescent labelling of the filaments allows for the monitoring of their activity during the assembly process. Thus, this system of molecular motors propelling functionalized filaments makes for an elegant minimalist system for the study of active self-assembly.

Here, we review the types of structures achieved with molecular motor-driven self-assembly focusing on whether or not the promises of active self-assembly were fulfilled. In particular, it has been claimed that active self-assembly can enable (1) faster assembly time, (2) larger structures and assembly of larger building blocks, and (3) more complex structures.<sup>4</sup> While it has been shown that motor-driven assembly does allow for larger structures to be built faster and that it is possible to assemble structures not attainable through diffusion-driven self-assembly,<sup>14</sup> we have not yet achieved the complexity or variety of structures that are available today using top-down fabrication methods.

## Cytoskeletal filaments and motor proteins

Microtubules (MT) and actin filaments (AF) are the main components of the cytoskeleton in cells, providing both mechanical support as well as serving as highways for motor proteins to transport vesicles and organelles around the cell.<sup>15</sup> The basic building blocks of MTs,  $\alpha\beta$ -tubulin heterodimers, join together end-to-end to form protofilaments, which in turn associate laterally to form hollow cylinders  $\sim 25$  nm in diameter (cite AkhmanovaSteinmetz2008) (Figure 2). *In vivo*, there are typically 13 protofilaments per MT, but protocols for making MTs *in vitro* result in various distributions of protofilament numbers per MT, depending on the polymerization conditions. MTs with 13 protofilaments have no pitch, whereas other protofilament numbers have either positive or negative pitch. For example, a 12-protofilament MT has a right-handed supertwist with a pitch of  $4.5 \pm 0.3$   $\mu\text{m}$  while a 14-protofilament MT has a left-handed supertwist with a pitch of  $-5.8 \pm 0.3$   $\mu\text{m}$  (cite ChretienWade1991, Ray1993) Each MT has a polarity with a distinct plus and minus end. *In vivo*, MTs are in

a dynamic equilibrium between assembly and disassembly, but in *in vitro* gliding assays, MTs are generally stabilized with paclitaxel (taxol) to prevent their disassembly.<sup>15</sup> AFs are polymers made from ATP-bound actin monomers. The actin monomers spiral around the axis of the filament with 1 turn every 37 nm (Figure 2).<sup>16</sup> They are also polar filaments with a plus and minus end. AFs are three hundred times more flexible than MTs, with a flexural rigidity of  $7.3 \times 10^{-26}$  N·m<sup>2</sup> (persistence length of about 10  $\mu\text{m}$ ) versus the MT's  $2.2 \times 10^{-23}$  N·m<sup>2</sup> (persistence length of about 6 mm).<sup>17</sup>

Two different classes of motor proteins bind to and move along MTs: kinesin and dynein. Kinesin motors serve diverse functions in cells ranging from vesicular transport (kinesin-I) to shortening MTs (MCAK). *In vitro* gliding assays generally use kinesin-I, which is a dimeric, processive, plus end directed motor that takes 8 nm steps (the length of tubulin dimer). Kinesin-I consists of an N-terminal ATP-binding motor domain, an  $\alpha$ -helical stalk, and a C-terminal tail domain, which is involved in cargo binding. Dynein, which is a minus end directed motor, is involved in retrograde motion of organelles and vesicles as well as motion of cilia and flagella. The motor domain consists of a heptameric wheel-like structure of 6 ATPase domains plus an additional C-terminal domain that are connected to the MT via a coiled-coil stalk.

AFs are associated with the myosin motor family. The structure of myosin is similar to that of kinesin, with a head domain that binds AFs and hydrolyzes ATP, a neck domain, and a tail domain connect to cargo or to other myosin subunits. While some myosin motors are like kinesin in that they are dimeric, other myosin motors are monomers, and only have a single head. All myosins except myosin VI are plus end directed. Not all myosin motors are processive

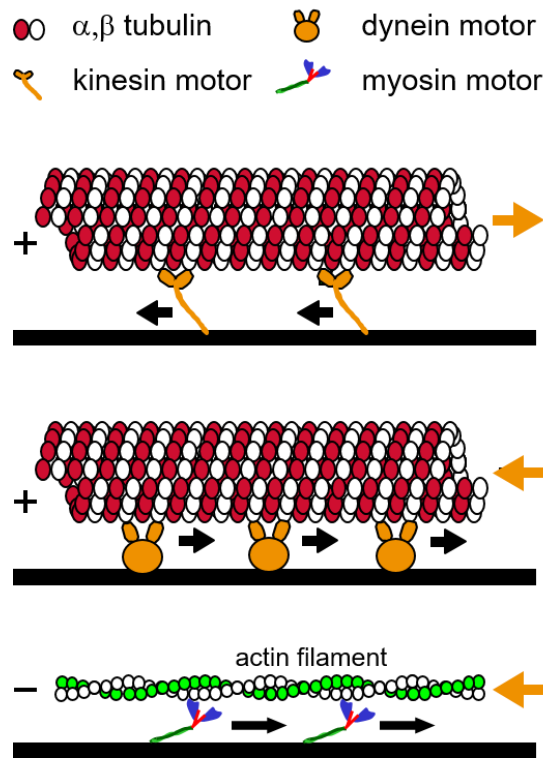


Figure 2: In gliding assays, cytoskeletal filaments, such as microtubules (MTs) and actin filaments (AFs), are transported by surface-adhered kinesins or dyneins, and myosins, respectively (not drawn to scale).

; motor processivity depends on the structure of the motor as well as the particular functions the motor plays *in vivo*, such as muscle contraction or vesicle transport (Figure 2).<sup>16</sup>

## Structures achieved via motor-driven assembly

### Filament bundles and wires

In gliding assays of cytoskeletal filaments functionalized with crosslinking agents such as biotin and streptavidin, the first step in the assembly of the propelled filaments is often the bundling of filaments through collision.<sup>18</sup> In this step, the motor-propelled filaments collide with each other, align, and are non-covalently cross-linked parallel to one another. In most cases, bundles are composed of several filaments, and their ends are not aligned (Figure 3). The fluorescence intensity of a bundle, taken to correspond to the number of filaments and varies along its length, reflecting the random attachment process. As motility continues in the flow cell, the bundles may grow in length or thickness, and may result in other structures (e.g. rings or spools). Determining how to create systems of filaments, motors, and cross-linkers which favor the assembly of linear arrays over other structures allows us to better control motor-driven self-assembly.

Control over the creation of MT bundles has been thoroughly explored over the last 10 years since the formation of extended bundles (or “wires”) was described as the result of an active self-assembly process.<sup>11, 19</sup> A number of factors such as rigidity, density, and velocity of MTs, as well as motor density were found to be involved.<sup>14, 20-22</sup> Unsurprisingly, it was found that stiffer MTs, prepared with guanylyl-( $\alpha$ ,  $\beta$ )-methylene-disphosphonate (GMPCPP), favored the production of linear bundles.<sup>22</sup> It was also shown that, because larger and longer bundles require more building blocks, the formation of longer bundles requires a higher initial density of MTs.<sup>14, 21, 22</sup> The MT gliding velocity was also found to affect the length of the assembled bundles; the longest MT bundle assembled with a relatively slow MT gliding velocity (0.1  $\mu$ m/s, compared to the maximum gliding speed of about 0.5  $\mu$ m/s).<sup>14</sup> At optimal conditions, MT bundles nearly 1 mm in length were assembled from MT building blocks approximately 10  $\mu$ m long.<sup>14</sup> While some studies show that having higher kinesin densities result in longer bundles,<sup>21</sup> other studies have suggested that higher kinesin densities may result in greater breakage of the MT bundles and thus result in shorter linear arrays.<sup>23, 24</sup> However, because the experimental conditions were not the same, (the studies cited used different variations of kinesin-I motors; ATP concentrations; observations times; and surface treatments), there are several possible explanations for these seemingly contradictory results. More studies are needed to determine how motor density affects bundle size. AFs have also been assembled into bundles *in vitro*, cross-linked by the protein

fascin. Unlike the streptavidin-biotin linkages, which may bind MT in an antiparallel fashion, fascin is a polar cross-linker which creates aligned AF bundles. The cross-linking of AFs via fascin results in higher stiffness of the AF bundles,<sup>25</sup> and given high enough fascin and AF concentrations, the AF bundles become sufficiently stiff to prevent curved trajectories, even when propelled by myosin motors. Over time, this system of AF, myosin, and fascin evolves to form straight, elongated bundles up to 50  $\mu$ m thick and centimeters long.<sup>26</sup> The increased stiffness may enable the use of these wires for patterning of cargo transport systems in nano-, micro-, and mesoscale chips.<sup>27</sup>

Without the aid of molecular motors, filaments may crosslink to each other due to electrostatic effects.<sup>28-30</sup> The filaments join end-to-end to create long wires rather than bundles. However, these wires were either not nearly as long as the ones created by Idan *et al.* through motor-driven self-assembly<sup>14, 29, 31</sup> or were formed over much longer timescales via 3-dimensional diffusion.<sup>30</sup> Furthermore, diffusion-driven self-assembly of streptavidin-covered MTs in two-dimensions, over similar timescales, could not result in such ordered structures, nor could it result in structures of such size.<sup>14</sup> Bundles formed through electrostatic interactions can, however, be made polar, depending on the crosslinker, and on a motor-coated surface, these bundles were motile with the velocity dependent on the degree of polarity.<sup>28</sup> In contrast, it is not possible to enforce polarity on MT gliding assays, which may be a drawback to the active self-assembly of MTs.

Bundled structures obtained from cytoskeletal filaments are particularly interesting because creating arrays of these bundles and motor proteins may enable us to develop force-multiplying structures similar to muscle. Furthermore, developing the control over the structural manipulation of bundles required such that they can assemble into arbitrary configurations over many length scales may be an attractive fabrication method for future devices, especially for directed transport of cargo in micro- or even nanofluidics. However, exact control over bundle size or location is yet to be realized.

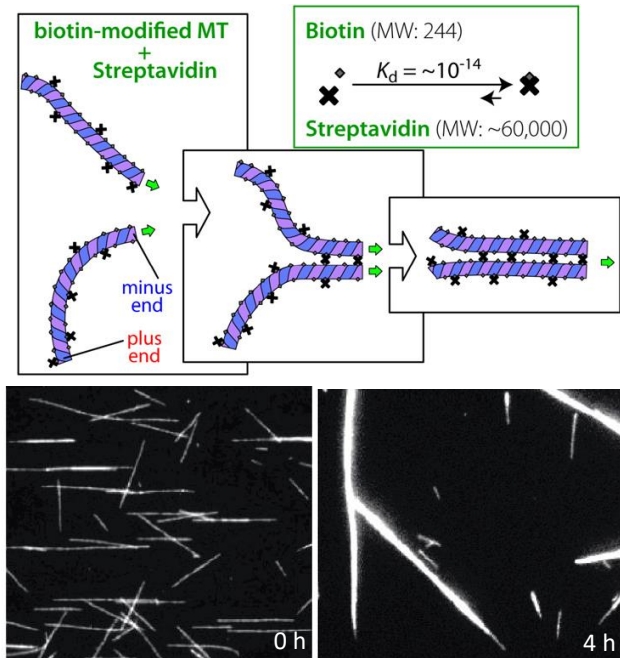


Figure 3: Active transport by surface-adhered kinesins leads to collisions between biotin-modified MTs partially coated with streptavidin and their cross-linking and assembly into bundles. The use of stiff MTs polymerized with GMPCPP effectively prevents the formation of spools. From Ref. 22 and Ref. 32.<sup>22,32</sup> Scale bar: 20  $\mu$ m.

#### Rings and spools

In addition to linear bundles, rings and spools are other characteristic structures which emerge from the active self-assembly of motor-driven cytoskeletal filaments. Here, we consider a ring to consist of a single filament or filament bundle that has cross-linked to itself in a closed loop, whereas a spool is formed from multiple filaments joined lengthwise. These circular structures have been first observed in MT/kinesin,<sup>9, 33</sup> then in AF/myosin,<sup>26</sup> and finally in MT/dynein systems<sup>34, 35</sup> (Figure 4).

Single AFs and AF bundles can crosslink into closed loops due to thermal fluctuations within a gliding assay as long as there is a sufficiently high concentration of the crosslinking agent fascin.<sup>26</sup> However, circular trajectories are not unique to closed loop structures; many “open rings” which are made of AFs cross-linked into an arc structure can also maintain a circular trajectory. As motility continues, more AFs are able to

collide with existing open and closed rings, cross-linking to them. If the assay continues for a sufficiently long time, most AFs in the system are incorporated into spools or rings, which continue to rotate, and the pattern of spools is considered “frozen” in a steady state.<sup>26</sup> Interestingly, if the non-polar cross-linking agent  $\alpha$ -actinin is used in place of fascin, spools are not assembled and instead the AFs separate into dilute and dense patches that actively contract.<sup>36</sup> This result is surprising as the crosslinking agent used in MT/kinesin systems (i.e., streptavidin) is also non-polar, and yet still able to support ring and spool formation, although this discrepancy could be due to other differences between the systems, such as the flexibility of the linker.

MTs are much stiffer than AFs, with a persistence length on the order of millimeters. Thus, MT spools are under considerable strain, storing up to  $10^5 k_B T$  of bending energy.<sup>9</sup> It has been shown that MT spools of small radii cannot arise from thermal fluctuations.<sup>31, 37</sup> Instead, they can be formed by strain-relaxation of MTs that crosslink into helices,<sup>33, 37, 38</sup> crosslinking of multiple MTs into closed loops,<sup>31</sup> or pinning of MT due to defects.<sup>24, 31</sup> Though all mechanisms are possible, pinning results in the tightest spools being formed because the motor proteins exert force on the MT, causing it to buckle in spite of its high stiffness. It is likely that pinning is the dominant cause for the initiation of MT spooling and determines the size distribution of the spools.<sup>24</sup>

There have been many studies on controlling the characteristic features of spools, revealing the roles of motor density, and length and rigidity of filaments. It was observed that higher motor densities lead to tighter spooling for MTs,<sup>24, 39</sup> but the opposite was noted in AF/myosin systems.<sup>36</sup> Stiffer MTs, prepared with GMPCPP in the tubulin polymerization buffer, have been observed to result in spools with larger diameters.<sup>40</sup> It has also been observed that longer MTs also result in larger spool diameters.<sup>40</sup> These results have been predicted by models and simulations.<sup>31</sup>

Adding MTs in successive stages into the flow cell was shown to be an effective way to tune the thickness of the spool as characterized by the difference between the outer and inner diameter of the spool.<sup>41</sup> It is also possible to control the direction of the rotational motion of the rings and spools. The supertwist of the MTs of greater or less than thirteen protofilaments can bias the rotation of the rings in either the clockwise or counterclockwise direction depending on whether

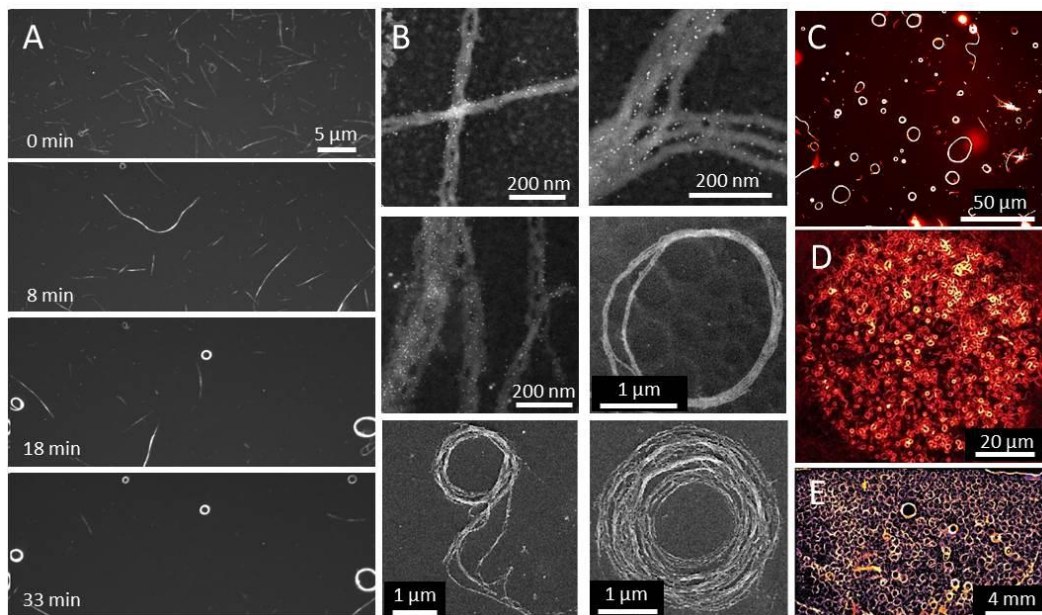


Figure 4: Fluorescence microscopy, scanning transmission electron microscopy (STEM), and scanning electron microscopy (SEM) images of circular structures created by self-assembly of molecular motors driven MTs. A) Formation of rings from kinesin driven biotinylated MTs. From Ref. 9.<sup>9</sup> B) STEM (top 4 panels) and SEM (2 lower panels) images of MT spools and bundles. Bright dots in STEM images are streptavidin coated-quantum dots. From Ref. 33.<sup>33</sup> C) Generally, the size of MT rings are distributed over a wide range as seen from the image of MT rings produced on a dynein coated surface. From Ref. 35.<sup>35</sup> D) MT rings were smaller with a more uniform size distribution when MT were self-assembled at an air-buffer interface without using any crosslinkers. From Ref. 42.<sup>42</sup> E) Vortices produced by self-assembly of dynein driven MTs. From Ref. 34.<sup>34</sup>

the supertwist is left- or right-handed; a left-handed supertwist results in preferential counterclockwise rotation while a right-handed supertwist results in preferential clockwise rotation.<sup>20, 33, 35, 38, 43</sup> Moreover, length and rigidity of the MT as well as the type of kinesin motor used in the assay can also significantly affect the bias of rotational direction of MT rings and spools.<sup>39</sup>

While thus far we have focused on rings and spools that are formed and stabilized by crosslinking, in systems with high filament densities, the filaments can also self-organize into rings, spools, and vortices through interactions with neighbouring filaments.<sup>34, 37</sup> Because these rings are not cross-linked, they are often transient features. However, if there is a sufficiently high density of filaments, due to crowding effects and interactions with nearest neighbors, a steady-state network of vortices may arise.<sup>34, 44</sup> This effect is more readily apparent in systems that use dynein because these motors are less flexible than kinesin motors; thus, using dynein forces, the MTs to remain in the same horizontal plane and interact with each other. It is necessary here to distinguish between self-organization, in which the formation of patterns and structures is maintained by the continuous flow of energy, and active self-assembly that uses energy flow in the formation of the structures, but not in the maintenance of them. These non-crosslinked rings formed in high-density filament assays are examples of the former.

MT rings and spools have also been formed at air-buffer interfaces in gliding assays without the use of streptavidin and biotin.<sup>42</sup> These spools formed at the air-buffer interface have

smaller circumferences than spools created in the traditional flow cells and a narrower size distribution. The necessary force for creating such small spooling radii in the MT can be explained by the hydrophilicity of the protein surface, which causes the MT to curve away from the air-buffer interface.

Rings and spools are of particular interest due to their ability to transform the linear translational motion of motors into rotational motion. Furthermore, their ordered arrangement decreases the entropy of the system, and in the case of MTs, these structures are under a great deal of strain. Thus, rings and spools have long been considered proof that non-equilibrium structures can self-assemble in systems where the motors enable access to a store of chemical energy. However, while recent studies have shown that ring and spool features can be controlled, the degree of control over these features remains limited. For example, size distribution is not yet uniform, nor is there perfect control over the rotation of the rings. Furthermore, while spools do show that strained structures can emerge from motor-driven self-assembly, other strained structures have not yet been realized. In these respects, much work remains to be done.

#### Network structures

In gliding assays with AFs with low fascin concentrations, relatively disorganized network structures emerged. It is believed that low fascin concentrations do not change pattern formation significantly, and thus a disorganized structure emerges. At sufficiently high AF densities, traveling density waves emerge as a self-organized structure.<sup>26</sup> In contrast,

gliding assays with MTs form networks when the ratio of the streptavidin crosslinker to biotin is high as well as the MT density. Because of the high streptavidin coverage, MTs are only able to bind to each other at isolated points rather than all along their lengths. Thus, no alignment of MT is observed. The MT networks also organize into areas of higher and lower densities, with average distances between intersection points of the MTs ranging from several to several tens of micrometers, and exhibit swarming behaviors.<sup>45</sup> Moreover, manipulation of interactions among the neighbouring microtubules at high densities, without using the crosslinking agents, can also give rise to self-organization into stable network structures.<sup>46</sup>

The gliding assay has also been used to assemble networks from materials other than cytoskeletal filaments. The force exerted by surface-adhered kinesin on MTs is sufficient for MTs crosslinked to lipids to pull lipid nanotubes from a multilamellar vesicle and create an interconnected lipid

be used to synthesize polymer nanotube networks, which display increased longevity compared to lipid nanotube networks but also exhibited decreased lateral diffusion of particles within the network.<sup>48</sup>

## Self-organization and self-assembly in 3D assays of motor proteins and filaments

Going beyond the 2D geometry of the gliding assay, other assays involving motor proteins and their associated filaments also can result in structure formation. By crosslinking the motor proteins rather than the filaments, structures other than spools and bundles, such as asters, vortices, and cilia-like bundles, can be created. Using a biotinylated kinesin and tetrameric streptavidin, multi-headed kinesin constructs can be assembled that can bind and walk on multiple MTs. In this configuration, kinesin is not attached to a substrate surface, and thus 3D rather than 2D structures can be created, in contrast to surface bound rings and bundles.

A minimalist system of stabilized MTs and multi-headed kinesin can self-assemble into asters, similar to meiotic and mitotic spindles found in cells; multi-headed kinesin constructs bind multiple MTs and each kinesin walks toward the plus end of each MT, resulting in the concentration of kinesin at the center of the aster with oriented MTs radiating out.<sup>49</sup> Alternatively, a minus-end directed motor construct, created with glutathione-S-transferease-nonclaret disjunctional fusion proteins, assembles asters with the opposite orientation with the MT minus-ends at the center.<sup>50</sup> In assays where both motor constructs are used, by tuning the concentrations of the components, it is possible to create a network of poles connected by aligned MTs.<sup>50</sup> Depending on the concentrations of the MTs and kinesin used, dynamic vortices can be formed instead of asters.<sup>49, 50</sup> A general theory for active viscoelastic materials made of polar filaments has been developed that predicts what structures will be formed as a function of the motor-generated stress and elastic moduli of the filaments.<sup>51</sup>

Control of the formation of asters can be achieved using molecular signals. By conjugating motors to DNA, instructions encoded in DNA sequences can then be used to associate the kinesin motors together to trigger aster formation or dissociate the motors to trigger disassembly. Further DNA sequences control the loading, concentration, and unloading of cargo from the asters. Potential applications of this system include color change (via concentration or distribution of pigment molecules) and concentration of reactants to speed up reactions or overcome high activation barriers.<sup>52</sup>

Cilia-like MT bundles have also been assembled and shown to exhibit cilia-like beating by Sanchez *et al* (Figure 6). These bundles are composed of surface stabilized MTs with one end tethered to a surface, biotin-kinesin cross-linked by streptavidin, and polyethylene glycol (PEG). While the multi-headed kinesin construct was required to aggregate the MTs into asters, the PEG provides a depletion force to enhance bundling. Then, the kinesin motors walk simultaneously on neighboring oppositely-oriented MTs in the bundle, causing

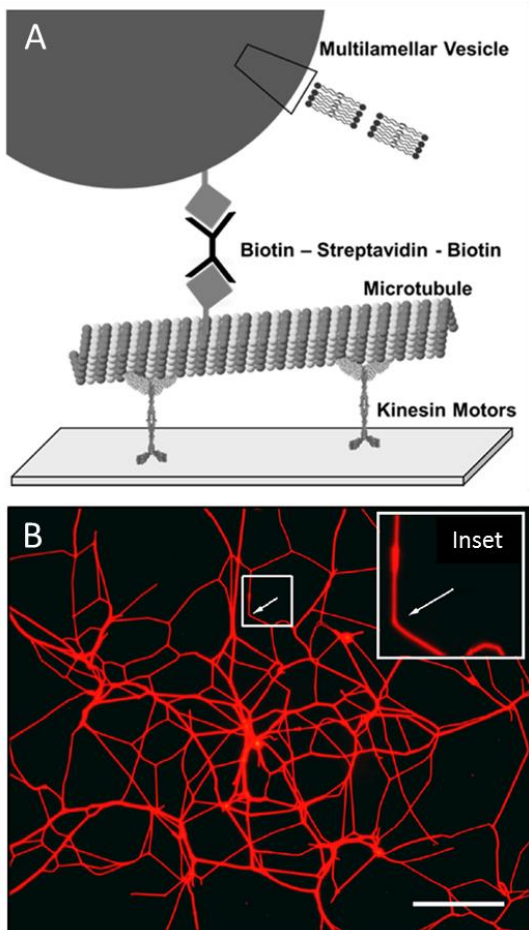
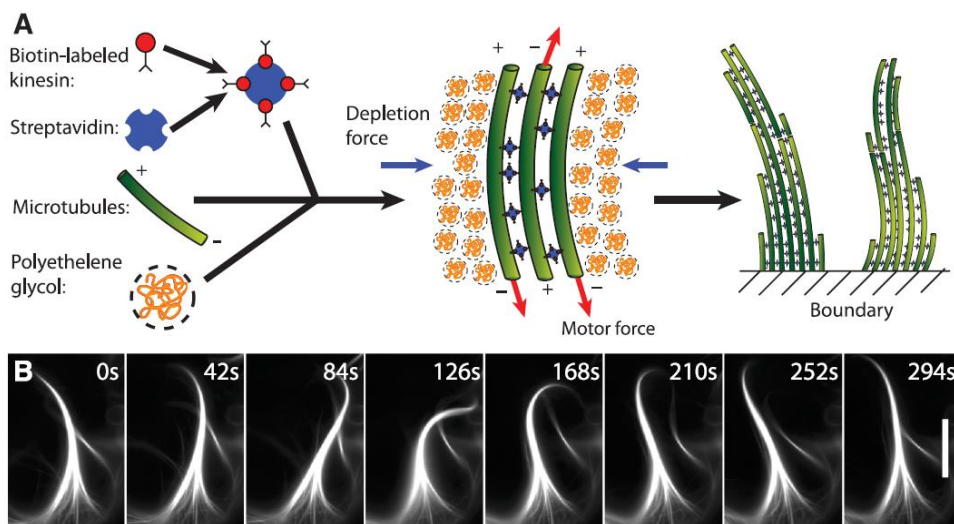


Figure 5. (A) Schematic of the assay in which nanotubes are pulled from multilamellar vesicles by MTs powered by surface-bound kinesin motors. (B) Example of lipid nanotube network. Scale bar: 50  $\mu$ m; inset shows free-standing kinked lipid nanotube (white arrow). From Ref. 46.<sup>47</sup> This system was used for capture and diffusive transport of nanomaterials, as demonstrated with quantum dots.<sup>47</sup> The same technique can

the MTs to slide relative to each other and resulting in beating of the bundle. They observe that dense fields of interacting active MT bundles exhibit synchronous beating behavior similar to metachronal waves seen in ciliary fields. As shown in Figure 6, this system demonstrates the potential of minimalist components to replicate complicated dynamic behaviors that mimic natural systems and potential application for fluid mixing and transport.<sup>53</sup>



assembly rules already reported in literature and offer new insights into our current understanding of active self-assembly.<sup>3</sup> To that end, phase diagrams summarizing the effects of various parameters on the final structures formed in MT-kinesin systems,<sup>21, 45, 54</sup> and AF-myosin systems<sup>26</sup> (Figure 7) have been created. However, as these phase diagrams are generated for quantities specific to these motor protein systems, it is not yet clear if and how these are translatable to a more general platform of active self-assembly.

The emergent structures and properties of the systems, however, do have ties to other biological phenomena and systems, and have potential for applications. For example, the asters created *in vitro* are similar in structure to mitotic spindles *in vivo*, and the wires and bundles are highly aligned structures similar to what is found in muscle and neurons. The vortices are more reminiscent of macroscopic phenomena such as swarming and flocking of self-propelled objects. Furthermore, vortices develop in gliding assays with high filament densities, which may be considered to be active nematic fluids, and many of the emergent properties of these high density assays, such as the generation of singularities and the large-scale flows, can be understood from that perspective. The behaviors of swarming and flocking have been studied extensively in robotics, which may provide further insights into motor protein-filament systems.<sup>55</sup>

The assembled structures, which are significantly different from the initial building blocks in size, shape and properties are potential candidates for various future applications in

## Understanding the dynamics of self-assembly

Due to the simplicity of the *in vitro* assays of motor proteins and cytoskeletal filaments, it was expected that these systems would provide some practical demonstrations of the self-

nanotechnology. For example, thick, long wires might be effective in elevating the efficiency of nanotransport systems, and designing artificial force generating systems. The circular structures formed may be employed in the future as micro-rotors, and network structures may become important for systems of molecular robots. However, low durability and short lifetime of assembled structures will be a major concern

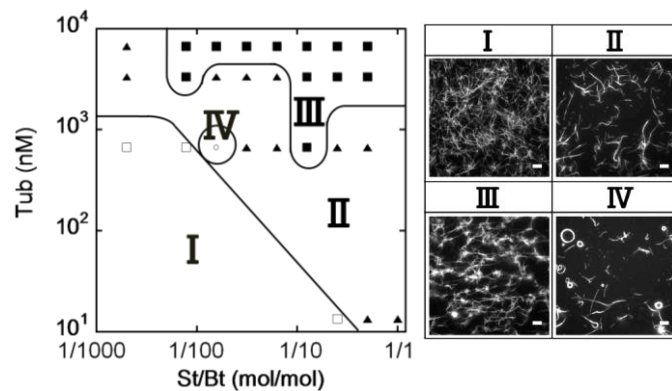


Figure 7. Phase diagram for self-assembly of MTs using streptavidin(St)-biotin(Bt) interaction showing the roles of crosslinker ratio (St/Bt) and tubulin concentration (Tub) in the morphological variations of assembled structures (left). Here, I, II, III and IV indicate phases of single filaments, bundles, networks and ring structures respectively, as shown by the fluorescence microscopy images (right). Scale bars: 10  $\mu$ m. From Ref. 44.<sup>45</sup>

for the adoption of these systems in nanotechnology. While the lifetime of these structures and systems has been dramatically prolonged by using an inert environment,<sup>56-58</sup> compared to the lifetime of current nanodevices powered by motor proteins, there is still much further to go.

## Conclusions

Over the past decade, much work has been done to elucidate the state space of motor-driven self-assembled structures. The effects of many system parameters have been uncovered, which enables the creation of systems favoring the assembly of specific structures and features above others. Looking back at the major claims of active or dynamic self-assembly, it has indeed been shown that by using motors to drive self-assembly processes, the assembly of building blocks can be accelerated and that larger, strained structures can be created. However, while control over their features has improved, there have been limited advances in increasing the variety of structures assembled; the library of achievable structures has not significantly expanded in these past 10 years. Furthermore, control over features is still quite inexact. It is clear that much more work remains to be done before we can fully harness the capabilities of active self-assembly.

## Acknowledgements

A.L. and H.H. gratefully acknowledge financial support from the US Army Research Office under grant W911NF-13-1-0390. V.V. and G.D.B gratefully acknowledge financial support by the U.S. Department of Energy, Office of Basic Energy Sciences, Division of Materials Sciences and Engineering (BES-MSE). Sandia National Laboratories is a multi-program laboratory managed and operated by Sandia Corporation, a wholly owned subsidiary of Lockheed Martin Corporation, for the U.S. Department of Energy's National Nuclear Security Administration under contract DE-AC04-94AL85000. A.M.R.K. and A.K. gratefully acknowledge support from Grant-in-Aid for Scientific Research on Innovative Areas "Molecular Robotics" (grant number 24104004) and Grant-in-Aid for JSPS Fellows from the Japan Society for the Promotion of Science.

## References

1. G. M. Whitesides and B. Grzybowski, *Science*, 2002, **295**, 2418-2421.
2. J.-M. Lehn, *PNAS*, 2002, **99**, 4763-4768.
3. M. Fialkowski, K. J. M. Bishop, R. Klajn, S. K. Smoukov, C. J. Campbell and B. A. Grzybowski, *Journal of Physical Chemistry B*, 2006, **110**, 2482-2496.
4. H. Hess, *Soft Matter*, 2006, **2**, 669-677.
5. E. Klavins, in *Control Problems in Robotics*, eds. A. Bicchi, H. Christensen and D. Prattichizzo, Springer, 2003, vol. 4, pp. 153-168.
6. N. Napp and E. Klavins, *Int. J. Robot. Res.*, 2011, **30**, 713-729.
7. M. Rubenstein, A. Cornejo and R. Nagpal, *Science*, 2014, **345**, 795-799.
8. J. V. I. Timonen, M. Latikka, L. Leibler, R. H. A. Ras and O. Ilkkala, *Science*, 2013, **341**, 253-257.
9. H. Hess and G. D. Bachand, *Materials Today*, 2005, **8**, 22-29.
10. J. M. Bauer, A. K. Boal, S. B. Rivera, R. G. Manley, G. D. Bachand, J. Liu, R. P. Manginell and B. C. Bunker, in *Micro Total Analysis Systems 2004, Vol 1*, eds. T. Laurell, J. Nilsson, K. Jensen, D. J. Harrison and J. P. Kutter, 2005, pp. 18-20.
11. H. Hess, J. Clemmens, C. Brunner, R. Doot, S. Luna, K.-H. Ernst and V. Vogel, *Nano Letters*, 2005, **5**, 629-633.
12. T. Nitta and H. Hess, *Nano Letters*, 2005, **5**, 1337-1342.
13. T. Nitta, A. Tanahashi, M. Hirano and H. Hess, *Lab on a Chip*, 2006, **6**, 881-885.
14. O. Idan, A. Lam, J. Kamcev, J. Gonzales, A. Agarwal and H. Hess, *Nano Letters*, 2012, **12**, 240-245.
15. J. Howard, *Mechanics of Motor Proteins and the Cytoskeleton*, Sinauer, Sunderland, MA, 2001.
16. B. Alberts, A. Johnson, J. Lewis, M. Raff, K. Roberts and P. Walter, *Molecular Biology of the Cell. Fourth Edition.*, 4 edn., Garland, New York, 2002.
17. F. Gittes, B. Mickey, J. Nettleton and J. Howard, *J. Cell Biol.*, 1993, **120**, 923-934.
18. J. D. Crenshaw, T. Liang, H. Hess and S. R. Phillpot, *Journal of Computational and Theoretical Nanoscience*, 2011, **8**, 1999-2005.
19. M. Bachand, A. M. Trent, B. C. Bunker and G. D. Bachand, *Journal of Nanoscience and Nanotechnology*, 2005, **5**, 718-722.
20. R. Kawamura, A. Kakugo, K. Shikinaka, Y. Osada and J. P. Gong, *Biomacromolecules*, 2008, **9**, 2277-2282.
21. R. Kawamura, A. Kakugo, Y. Osada and J. P. Gong, *Nanotechnology*, 2010, **21**, 145603.
22. R. Kawamura, A. Kakugo, Y. Osada and J. P. Gong, *Langmuir*, 2010, **26**, 533-537.
23. E. L. P. Dumont, C. Do and H. Hess, *Nature Nanotechnology*, 2015, **10**, 166-169.
24. A. T. Lam, C. Curschellas, D. Krovvidi and H. Hess, *Soft Matter*, 2014, **10**, 8731-8736.
25. M. M. A. E. Claessens, M. Bathe, E. Frey and A. R. Bausch, *Nature Materials*, 2006, **5**, 748-753.
26. V. Schaller, C. A. Weber, B. Hammerich, E. Frey and A. R. Bausch, *PNAS*, 2011.
27. H. Takatsuki, K. M. Rice, S. Asano, B. S. Day, M. Hino, K. Oiwa, R. Ishikawa, Y. Hiratsuka, T. Q. P. Uyeda, K. Kohama and E. R. Blough, *Small*, 2010, **6**, 452-457.
28. A. Kakugo, K. Shikinaka, N. Takekawa, S. Sugimoto, Y. Osada and J. P. Gong, *Biomacromolecules*, 2005, **6**, 845-849.
29. K. Y. Kwon, K. L. Wong, G. Pawin, L. Bartels, S. Stolbov and T. S. Rahman, *Physical Review Letters*, 2005, **95**, 166101.
30. M. Bachand, N. F. Bouxsein, S. Cheng, S. J. von Hoyningen-Huene, M. J. Stevens and G. D. Bachand, *RSC Advances*, 2014, **4**, 54641-54649.
31. I. Luria, J. Crenshaw, M. Downs, A. Agarwal, S. B. Seshadri, J. Gonzales, O. Idan, J. Kamcev, P. Katira, S. Pandey, T. Nitta, S. R. Phillpot and H. Hess, *Soft Matter*, 2011, **7**, 3108-3115.
32. R. Kawamura, A. Kakugo, K. Shikinaka, Y. Osada and J. P. Gong, *Smart Mater Struct*, 2011, **20**.

33. H. Q. Liu, E. D. Spoerke, M. Bachand, S. J. Koch, B. C. Bunker and G. D. Bachand, *Advanced Materials*, 2008, **20**, 4476-4481.

34. Y. Sumino, K. H. Nagai, Y. Shitaka, D. Tanaka, K. Yoshikawa, H. Chate and K. Oiwa, *Nature*, 2012, **483**, 448-452.

35. M. Ito, A. M. R. Kabir, D. Inoue, T. Torisawa, Y. Toyoshima, K. Sada and A. Kakugo, *Polymer Journal*, 2014, **46**, 220-225.

36. V. Schaller, K. M. Schmoller, E. Karakoese, B. Hammerich, M. Maier and A. R. Bausch, *Soft Matter*, 2013, **9**, 7229-7233.

37. L. Liu, E. Tuzel and J. L. Ross, *J Phys-Condens Mat*, 2011, **23**.

38. F. Ziebert, H. Mohrbach and I. M. Kulic, *Physical Review Letters*, 2015, **114**.

39. S. Wada, A. M. R. Kabir, R. Kawamura, M. Ito, D. Inoue, K. Sada and A. Kakugo, *Biomacromolecules*, 2015, **16**, 374-378.

40. S. Wada, A. M. R. Kabir, M. Ito, D. Inoue, K. Sada and A. Kakugo, *Soft Matter*, 2015, **11**, 1151-1157.

41. D. Inoue, A. M. R. Kabir, H. Mayama, J. P. Gong, K. Sada and A. Kakugo, *Soft Matter*, 2013, **9**, 7061-7068.

42. A. M. R. Kabir, S. Wada, D. Inoue, Y. Tamura, T. Kajihara, H. Mayama, K. Sada, A. Kakugo and J. P. Gong, *Soft Matter*, 2012, **8**, 10863-10867.

43. A. Kakugo, A. M. R. Kabir, N. Hosoda, K. Shikinaka and J. P. Gong, *Biomacromolecules*, 2011, **12**, 3394-3399.

44. V. Schaller, C. Weber, C. Semmrich, E. Frey and A. R. Bausch, *Nature*, 2010, **467**, 73-77.

45. Y. Tamura, R. Kawamura, K. Shikinaka, A. Kakugo, Y. Osada, J. P. Gong and H. Mayama, *Soft Matter*, 2011, **7**, 5654-5659.

46. D. Inoue, B. Mahmot, A. M. R. Kabir, T. I. Farhana, K. Tokuraku, K. Sada, A. Konagaya and A. Kakugo, *Nanoscale*, 2015.

47. N. F. Bouxsein, A. Carroll-Portillo, M. Bachand, D. Y. Sasaki and G. D. Bachand, *Langmuir*, 2013, **29**, 2992-2999.

48. W. F. Paxton, N. F. Bouxsein, I. M. Henderson, A. Gomez and G. D. Bachand, *Nanoscale*, 2015, **7**, 10998-11004.

49. F. J. Nedelev, T. Surrey, A. C. Maggs and S. Leibler, *Nature*, 1997, **389**, 305-308.

50. T. Surrey, F. Nedelev, S. Leibler and E. Karsenti, *Science*, 2001, **292**, 1167-1171.

51. K. Kruse, J. F. Joanny, F. Julicher, J. Prost and K. Sekimoto, *Physical Review Letters*, 2004, **92**.

52. A. J. M. Wollman, C. Sanchez-Cano, H. M. J. Carstairs, R. A. Cross and A. J. Turberfield, *Nature Nanotechnology*, 2014, **9**, 44-47.

53. T. Sanchez, D. Welch, D. Nicastro and Z. Dogic, *Science*, 2011, **333**, 456-459.

54. H. Liu and G. D. Bachand, *Soft Matter*, 2011, **7**, 3087-3091.

55. V. Schaller and A. R. Bausch, *Proceedings of the National Academy of Sciences of the United States of America*, 2013, **110**, 4488-4493.

56. A. M. R. Kabir, D. Inoue, A. Kakugo, K. Sada and J. P. Gong, *Polymer Journal*, 2012, **44**, 607-611.

57. A. M. R. Kabir, D. Inoue, A. Kakugo, A. Kamei and J. P. Gong, *Langmuir*, 2011, **27**, 13659-13668.

58. V. VanDelinder and G. D. Bachand, *Analytical Chemistry*, 2014, **86**, 721-728.